21st Australasian Fluid Mechanics Conference
Adelaide, Australia
10-13 December 2018

Shear Stresses on Beds with Large Roughness Elements

V. Etminan[1,2], M. Conde-Frias[2,3], M. Abdolahpour[2], M. Ghisalberti[1,4] and R. Lowe[2,3,5]

[1]Department of Civil, Environmental and Mining Engineering,
The University of Western Australia, Perth, WA 6009, Australia

[2]Oceans Graduate School,
The University of Western Australia, Perth, WA 6009, Australia

[3]ARC Centre of Excellence for Coral Reef Studies,
The University of Western Australia, Perth, WA 6009, Australia

[4]Department of Infrastructure Engineering,
The University of Melbourne, Parkville, Victoria 3010, Australia

[5]UWA Oceans Institute,
The University of Western Australia, Perth, WA 6009, Australia

Abstract

Large bed roughness such as vegetation, gravels, ripples, etc. alters many benthic processes including sediment transport which, in turn, significantly affects the bed stability, channel morphology. Models to predict the onset and rates of sediment transport in environmental systems are conventionally related to the bed shear stress. Several methods exist to estimate the shear stress on bare beds but none of them are strictly applicable to beds with large roughness, predominantly due to the large impact roughness can have on the near-bed mean and turbulent flow structure. Recently, a Linear Stress Model (LSM) has been proposed to predict the spatially-averaged bed shear stress in vegetated flows. However, while the distribution of shear stress is uniform over bare beds, it is highly spatially-variable in the presence of large roughness elements. A full understanding of this variability is essential for predicting the extent and location of sediment mobilisation. In this study, high resolution computational fluid dynamics simulations were used to describe the spatial variation of shear stress on vegetated beds across a wide range of canopy densities (from 1.6% to 25% by area) and Reynolds numbers (from 200 to 1340). To complement the numerical results, bed shear stress distributions were measured in a laboratory flume using Particle Image Velocimetry (PIV). The numerical and experimental results reveal that, in sparse canopies, bed shear stress distributions become approximately uniform (and close to that predicted by the LSM) far from the canopy stems. However, the bed shear stress is highly variable throughout denser canopies. In addition, it is shown that presence of vegetation significantly reduces the spatially-averaged bed shear stress compared to that of a bare bed for given channel and flow conditions. The results of this study provide a foundation for improving predictions of sediment transport in vegetated river beds and current-dominated coastal regions where direct measurement of the full (spatially-averaged) bed shear stress field is near impossible.

Introduction

Large bed roughness such as vegetation, gravels, ripples, etc. has a significant influence on the flow in rivers, floodplains and coastal areas. The roughness elements create velocity and turbulence intensity profiles near the bed that deviate from those in flows over bare beds [1-3]. As a consequence, sediment transport characteristics can be significantly altered when flow moves over rough beds [4]. The rate of sediment transport can considerably affect the vegetation propagation, channel stability [5, 6], and turbidity of fish habitats [7, 8] which emphasises the importance of reliable formulations for predicting sediment transport in the presence of large bed roughness.

The onset and rates of sediment transport are typically related to the bed shear stress τ_b. In bare-bed channels, the bed shear stress can be estimated using several methods such as fitting the mean velocity profile based on a logarithmic Law of the Wall (Figure 1a), by the water surface slope method which relies on a momentum balance, by extrapolating near-bed turbulent stress and using the empirical relation between turbulent kinetic energy (TKE) and bed shear stress [9]. None of these methods are strictly applicable to beds with large roughness, due partly to the impact of roughness on the velocity profile and turbulence production [10]. In search of a predictive tool for vegetated bed shear stress, Yang, et al. [10] proposed a Linear Stress Model (LSM) that defines a viscous layer with a thickness of H_v immediately above the bed, within which the turbulent stress is negligible and the viscous stress decreases linearly with distance from the bed, resulting in a parabolic velocity profile (Figure 1b). In the upper water column ($z \geq H_v$), the streamwise velocity is assumed to be vertically-uniform such that viscous stress is negligible. The LSM velocity profile is expressed as

$$\langle \bar{u} \rangle = \begin{cases} \dfrac{\langle u_* \rangle_{LSM}^2}{\nu}\left(z - \dfrac{z^2}{2H_v}\right), & z \leq H_v \\ \dfrac{\langle u_* \rangle_{LSM}^2 H_v}{2\nu}, & z \geq H_v \end{cases} \quad (1)$$

where ν is kinematic viscosity and overbar and $\langle\ \ \rangle$ indicate temporal and spatial averaging, respectively. It has been shown that equation (1) agree very well with the experimental [10] and numerical [11] velocity profiles, using both the friction velocity $\langle u_* \rangle_{LSM} = \sqrt{|\overline{\tau_b}|/\rho}$ (with ρ indicating fluid density) and H_v as fitting parameters. Furthermore, Etminan, et al. [11] used TKE budget near bed to propose a reliable formulation for predicting H_v which only requires roughness characteristics and flow velocity as input. Therefore, $\langle u_* \rangle_{LSM}$ can be readily estimated using equation (1).

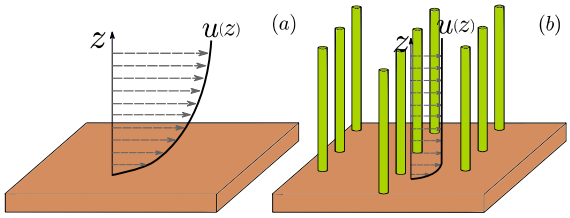

Figure 1 The velocity profile $u(z)$ in (a) bare beds and (b) beds with large roughness elements.

In addition to the spatially-averaged bed shear stress (or friction velocity) values, understanding bed shear stress distributions is also very important as, unlike bare beds, they are highly spatially-variable in the presence of roughness [4]. The onset of sediment resuspension and higher rates of sediment transport are both more likely to occur locally in the regions with higher bed shear stress. In case of vegetated beds, conventional experimental studies of bed shear stresses have usually adopted one of two approaches: (1) measuring the velocity profiles at a limited number of points within the canopy [10] or (2) estimating values by measuring the energy slope (total flow resistance) and subtracting the predicted vegetative drag [12, 13]. Neither of these approaches is capable of effectively capturing the spatial variability of bed shear stress. In contrast, accurate Particle Image Velocimetry (PIV) measurements and high-resolution computational fluid dynamics (CFD) simulations can provide direct and detailed measurements of shear stress over an entire bed.

In this study, we employ Large Eddy Simulations (LES) and PIV to investigate the bed shear stresses on beds with large roughness, modelled here as staggered arrays of rigid cylinders. First, we evaluate the performance of an improved Linear Stress Model in estimating the spatially averaged friction velocity in presence of roughness. We then look into the spatial variability of bed shear stress that has important implications for understanding sediment transport patterns.

Methodology

Numerical Methods

The numerical results presented in this study are based on the numerical approach detailed in [14] and [11], with only a summary of that approach included here. Three-dimensional Large Eddy Simulations were used to model the flow through large bed roughness elements modelled as arrays of rigid circular cylinders. All simulations were conducted using OpenFOAM version 2.3.0, which has been widely used for modeling flow around bluff bodies [15-18]. Four rigid emergent cylinders in a staggered arrangement were included within the computational domain and, to mimic an infinite array of cylinders, cyclic boundary conditions were imposed in both the streamwise and spanwise directions (Figure 2c). At the bed and cylinder surfaces, a no-slip condition was applied. In all simulations, the cell sizes adjacent to solid surfaces (i.e., around each cylinder and at the bed) were chosen such that the first grid point was well within the viscous sublayer. The array solid fraction or density λ $(= (\pi/2)(d/s)^2$ where d is cylinders diameter), was varied by adjusting the cylinder spacing, s (Figure 2c) such that $\lambda = 0.016$, 0.04, 0.08, 0.12, 0.20, and 0.25. A mean pressure gradient was imposed in the streamwise direction to drive the flow at the specified pore velocities U_p $(= Q/Wh(1-\lambda)$, where Q is the channel discharge, W is the channel width and h is the flow depth) corresponding to four Reynolds numbers ($Re_p = U_p d/\nu = 200$, 500, 1000 and 1340). These Reynolds numbers are typical of those in flows through aquatic vegetation [19].

Experimental Setup

The experiments were carried out in a 2m × 0.40m × 0.40m glass-sided flume. Rigid cylinders with diameter of $d =$ 6.4mm arranged in a staggered configuration were used to simulate bed roughness elements (Figure 1a and b). The still water depth ($h = 10$cm) was kept constant throughout the experiments. Spatial variations of stream-wise velocity components were obtained within viscous sublayer using PIV for three different Reynolds numbers ($Re_p = 190$, 210 and 260) and one array density ($\lambda = 0.04$). Pliolite AC80 with nominal diameter of 52 – 75 μm was used as seeding particles. A Prosilica GT2450 camera with a resolution of 2448 × 2050 pixels was used to capture the images. The frames were recorded for 5 min at frame rate of 36 fps, covering a region of 11.4 × 53.7 mm^2 (indicated by dashed lines in Figure 1b). The recorded pictures were post-processed using the free software PIVlab [20]. For the correlation algorithm, the direct Fourier transform correlation with multiple passes and deforming windows was implemented.

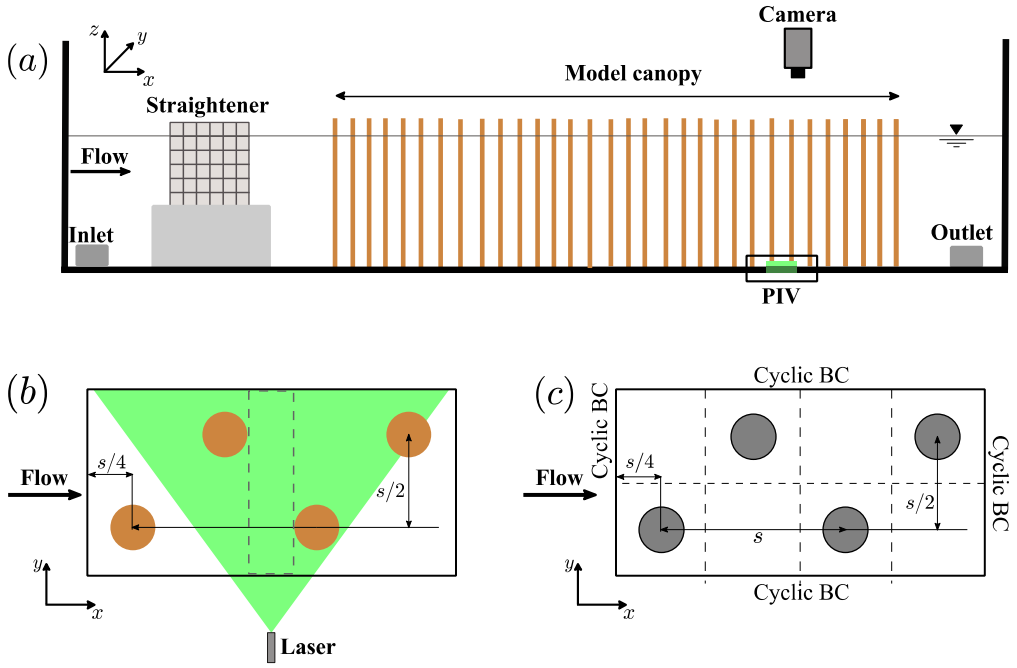

Figure 2 (a) Schematic view of the experimental configuration in the flume; (b) The region where experimental measurements were made indicated by dashed lines and (c) Numerical domain.

Model Data Analysis

The friction velocity was calculated using two methods. First, the local friction velocity based on near-bed velocity gradient was calculated as

$$u_* = \sqrt{|\overline{\tau_b}|/\rho} \tag{2}$$

where $\overline{\tau_b}$ is derived from the temporally-averaged stream-wise velocity profile:

$$\overline{\tau_b} = \mu\left(\frac{\partial \bar{u}}{\partial z}\right)_{z=0} \tag{3}$$

with μ as the dynamic viscosity. The spatially-averaged friction velocity based on this method is denoted as $\langle u_* \rangle$. Second, the spatially-averaged friction velocity based on LSM method was calculated as

$$\langle u_* \rangle_{LSM} = U_p \sqrt{\frac{2}{Re_{p,H_v}}} \tag{4}$$

which is derived from equation (1) with $Re_{p,H_v} = U_p H_v/\nu$. In addition, the height of the viscous layer H_v was determined using the equation proposed by [11]:

$$H_v = 5.15\sqrt{\frac{\nu\langle \bar{k} \rangle}{C_{d,c}^{form} a U_c^3}} \tag{5}$$

where $\langle \bar{k} \rangle$ is turbulent kinetic energy (calculated based on equation (4.1) in [21]), $C_{d,c}^{form}$ is the canopy form drag (calculated based on equation (10) in [11]), a is canopy frontal area $(= d/0.5s^2)$ and U_c is constricted cross-section velocity $(= U_p(1-\lambda)/(1-\sqrt{2\lambda/\pi}))$.

Results

To examine the performance of the revised LSM proposed by Etminan, et al. [11], the spatially-averaged friction velocity $\langle u_* \rangle_{LSM}$ was calculated for the numerical and experimental flow scenarios using the procedure described above. The excellent agreement ($R^2 = 0.97$) between the predicted values of $\langle u_* \rangle_{LSM}$ and the measured numerical and experimental values $\langle u_* \rangle$ (Figure 3) demonstrates the accuracy of the revised LSM. It is also evident that friction velocity increases with canopy density.

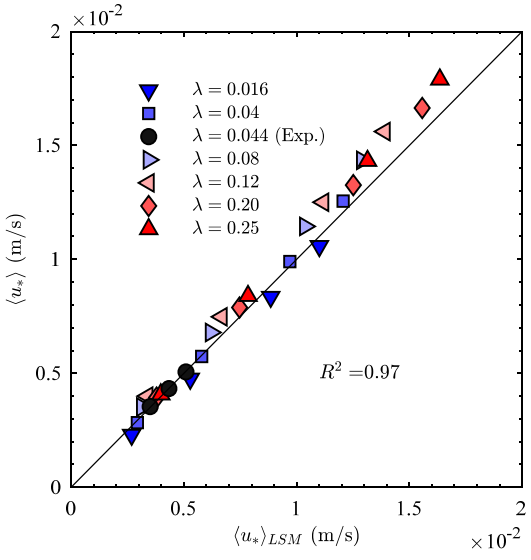

Figure 3 The excellent agreement between numerically calculated (colour symbols) and experimentally measured (black circles) values of spatially averaged friction velocity $\langle u_* \rangle$ and those calculated using the revised LSM $\langle u_* \rangle_{LSM}$.

The normalized friction velocity ($u_*/\langle u_* \rangle$) distributions display high spatial-variability (Figure 4). Locally there is a small area with negative shear stress immediately upstream of each cylinder (indicated in blue in Figure 4), as a result of the horseshoe vortex formation at the base of cylinders. There is another area with negative shear stress downstream of each cylinder due to the recirculation in the wake region. Small areas with elevated stress on each side of the cylinder (indicated in dark red in Figure 4) are due to the local contraction of streamlines. However, we note that all these areas with elevated or negative shear stress become constrained by neighbouring cylinders in the streamwise and spanwise directions as the canopy density increases.

Although for sparse canopies the friction velocity distributions eventually become approximately uniform far from the cylinders (indicated in white in Figure 4), $u_*/\langle u_* \rangle$ is highly variable throughout denser arrays (Figure 4c). Such substantial spatial variability of bed shear stresses has important implications for understanding sediment transport patterns and also for conducting experimental measurements of bed shear stresses in the presence of large roughness elements. For example, there can be large errors associated with measuring the bed shear stress at only a limited number of accessible locations within aquatic canopies, especially in denser canopies.

Finally, it should be noted that if the results depicted in Figure 3 are not interpreted correctly, one may conclude that increasing roughness density in channels increases the bed shear stress. However, for a channel with fixed flow rate, this is not the case. This is because higher vegetation density results in increased flow resistance, a greater flow depth, lower U_p and consequently lower friction velocity. As an example, we consider a channel with given flow rate Q $(0.008\,\mathrm{m}^3/\mathrm{s})$, bed friction factor f (0.04) and channel bed slope s_b (0.0005). Using the revised LSM combined with a momentum balance, the variation of flow depth h and spatially-averaged LSM friction velocity $\langle u_* \rangle_{LSM}$ with canopy density λ are demonstrated in Figure 5. For the densest canopy, the flow depth increases by a factor of ~11 across the range of canopy densities considered here. This results in a corresponding decrease in the pore velocity U_p, such that the friction velocity in a $\lambda = 0.25$ canopy is less than half of that in a $\lambda = 0.01$ canopy. Indeed, the shear stress in this dense canopy is almost 70 times less than that over a bare bed in the same channel.

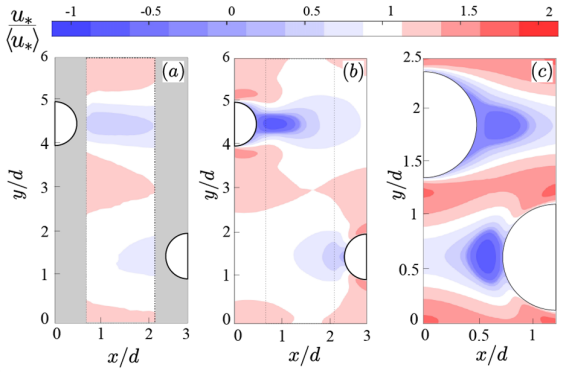

Figure 4 The spatial variability of dimensionless friction velocity $u_*/\langle u_* \rangle$ calculated based on (a) experimental measurements at $Re_p = 260$ and $\lambda = 0.044$ and also numerical results at $Re_p = 500$ and (b) $\lambda = 0.04$ and (c) $\lambda = 0.25$.

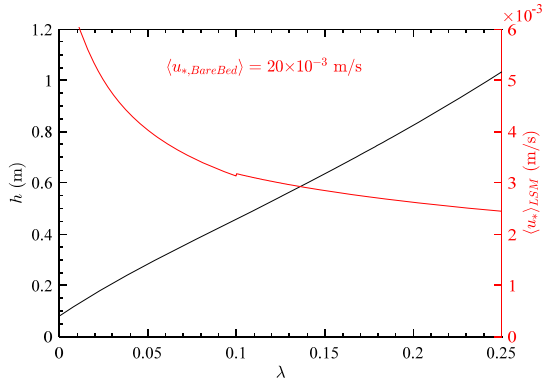

Figure 5 The variations of flow depth h and spatially-averaged LSM friction velocity $\langle u_* \rangle_{LSM}$ with the canopy density λ in a wide channel with flow rate of 0.008 m^3/s, a bed friction factor of 0.04 and bed slope of 0.0005

Conclusions

In this study, the impact of the large bed roughness on bed shear stress was evaluated using high resolution Computational Fluid Dynamics (CFD) and experimental measurements. The Linear Stress Model (LSM) originally proposed by Yang, et al. [10] and improved by Etminan, et al. [11], was found to be a reliable tool to estimate bed shear stress across a wide range of flow and roughness characteristics, modelled here as arrays of rigid numerical results revealed that far from the cylinders, bed shear stress distributions become approximately uniform (and close to the spatially-averaged value predicted by the LSM) for low array densities. The distribution of bed shear stress in denser arrays, however, is highly variable. Thus, estimating spatially-averaged bed shear stress from a limited number of local measurements (as have been done in previous studies) may cause a non-negligible impact on the prediction of sediment transport in beds with large roughness elements. The improved understanding of the near-bed flow and shear stress distribution obtained here provide a step towards a more accurate prediction of sediment transport in beds with large roughness and thus, an improved management of these valuable ecosystems.

Acknowledgments

V. E., R. L. and M. G. acknowledge support for the project provided by the Western Australian Marine Institute (WAMSI) Dredging Science Node (Theme 2/3). M. C. was supported by an Australian Government International Research Training Program Fee Offset Scholarship. Computational resources for the project were provided by the Pawsey Supercomputing Centre with funding from the Australian Government and the Government of Western Australia.

References

[1] Liu, D., Diplas, P., Fairbanks, J. D. and Hodges, C. C. An experimental study of flow through rigid vegetation. *Journal of Geophysical Research: Earth Surface*, 113, F4 (2008), 1283-1308.

[2] Nepf, H. M. Drag, turbulence, and diffusion in flow through emergent vegetation. *Water Resources Research*, 35, 2 (1999), 479-489.

[3] Yager, E. and Schmeeckle, M. The influence of vegetation on turbulence and bed load transport. *Journal of Geophysical Research: Earth Surface*, 118, 3 (2013), 1585-1601.

[4] Nepf, H. M. Hydrodynamics of vegetated channels. *Journal of Hydraulic Research*, 50, 3 (2012), 262-279.

[5] Afzalimehr, H. and Dey, S. Influence of bank vegetation and gravel bed on velocity and Reynolds stress distributions. *International Journal of Sediment Research*, 24, 2 (2009), 236-246.

[6] Pollen-Bankhead, N. and Simon, A. Hydrologic and hydraulic effects of riparian root networks on streambank stability: Is mechanical root-reinforcement the whole story? *Geomorphology*, 116, 3 (2010), 353-362.

[7] Lenhart, C. F. *The influence of watershed hydrology and stream geomorphology on turbidity, sediment and nutrients in tributaries of the Blue Earth River*. University of Minnesota, Minnesota, USA, 2008.

[8] Montakhab, A., Yusuf, B., Ghazali, A. and Mohamed, T. Flow and sediment transport in vegetated waterways: a review. *Reviews in Environmental Science and Bio/Technology*, 11, 3 (2012), 275-287.

[9] Biron, P. M., Robson, C., Lapointe, M. F. and Gaskin, S. J. Comparing different methods of bed shear stress estimates in simple and complex flow fields. *Earth Surface Processes and Landforms*, 29, 11 (2004), 1403-1415.

[10] Yang, J. Q., Kerger, F. and Nepf, H. M. Estimation of the bed shear stress in vegetated and bare channels with smooth beds. *Water Resources Research*, 51, 5 (2015), 3647-3663.

[11] Etminan, V., Ghisalberti, M. and Lowe, R. J. Predicting bed shear stresses in vegetated channels. *Water Resources Research*, 54 (2018).

[12] Jordanova, A. A. and James, C. Experimental study of bed load transport through emergent vegetation. *Journal of Hydraulic Engineering*, 129, 6 (2003), 474-478.

[13] Kothyari, U. C., Hayashi, K. and Hashimoto, H. Drag coefficient of unsubmerged rigid vegetation stems in open channel flows. *Journal of Hydraulic Research*, 47, 6 (2009), 691-699.

[14] Etminan, V., Lowe, R. J. and Ghisalberti, M. A new model for predicting the drag exerted by vegetation canopies. *Water Resources Research*, 53, 4 (2017), 3179–3196.

[15] Lloyd, T. P. and James, M. Large eddy simulations of a circular cylinder at Reynolds numbers surrounding the drag crisis. *Applied Ocean Research* (2015).

[16] Lysenko, D. A., Ertesvåg, I. S. and Rian, K. E. Large-eddy simulation of the flow over a circular cylinder at reynolds number 3900 using the openfoam toolbox. *Flow, Turbulence and Combustion*, 89, 4 (2012), 491-518.

[17] Lysenko, D. A., Ertesvåg, I. S. and Rian, K. E. Large-eddy simulation of the flow over a circular cylinder at Reynolds number 2×10^4. *Flow, turbulence and combustion*, 92, 3 (2014), 673-698.

[18] Sidebottom, W., Ooi, A. and Jones, D. A Parametric Study of Turbulent Flow Past a Circular Cylinder Using Large Eddy Simulation. *Journal of Fluids Engineering*, 137, 9 (2015), 091202.

[19] Nepf, H. M. *Flow over and through biota*. Academic Press., City, 2011.

[20] Thielicke, W. and Stamhuis, E. PIVlab–towards user-friendly, affordable and accurate digital particle image velocimetry in MATLAB. *Journal of Open Research Software*, 2, 1 (2014).

[21] Tanino, Y. and Nepf, H. M. Lateral dispersion in random cylinder arrays at high Reynolds number. *Journal of Fluid Mechanics*, 600 (2008), 339-371.